Inclusive Δ^{++}(1232) production in $\pi^- p$ interactions at 15 GeV/c

F. Barreiro, O. Benary,* J. E. Brau, J. Grunhaus,† E. S. Hafen, R. I. Hulsizer, U. Karshon,‡ V. Kistiakowsky,
A. Levy,† A. Napier, I. A. Pless, J. P. Silverman, P. C. Trepagnier, J. Wolfson,§ and R. K. Yamamoto

Laboratory for Nuclear Science, Massachusetts Institute of Technology, Canbridge, Massachusetts 02139

(Received 29 August 1977)

We present in this paper a study of the Δ^{++}(1232) inclusive production for momentum transfer squared to the target proton, $|t| < 1$ (GeV/c)^2. We have investigated the production mechanism of the Δ^{++} by measuring its density matrix elements as a function of t and of the missing mass squared, M_X^2, and by carrying out a triple-Regge analysis. For $|t| < 0.4$ (GeV/c)^2, the Δ^{++} production mechanism is consistent with one-pion exchange. We have also studied the average charged multiplicity recoiling from the Δ^{++} as a function of M_X^2, for $|t| < 0.4$ (GeV/c)^2. The study yields information about the $\pi^- \pi^-$ average charged multiplicity.

I. INTRODUCTION

It has been shown recently that inclusive Δ^{++} production may be described by two apparently different mechanisms which result in the same experimental observations.[1,2] A study of the reaction

$$\pi^- p \to \Delta^{++}(1232)X^{--} \tag{1}$$

(where X^{--} stands for anything) at 147 GeV/c has shown that the properties of inclusive Δ^{++} production are consistent with both one-pion exchange at the lower vertex and resonance formation at that vertex, which then decays into $\Delta^{++}\pi^-$ (see Fig. 1).[1] The former interpretation has been used for the description of Δ^{++} inclusive production in the energy range 8–300 GeV/c in pp,[3] $\pi^+ p$,[4] $\pi^- p$,[5] and $K^- p$ [6] interactions.

In an earlier publication studying reaction (1) at 15 GeV/c, we have shown that the experimental results are consistent with what would be expected

FIG. 1. Diagrams describing Δ^{++} production via (a) single-exchange and (b) double-exchange mechanisms.

if the Δ^{++} were a decay product of a diffractively produced higher-mass object, a main component of which is a low-mass $\Delta^{++}\pi^-$ system.[7] In the present paper we study the inclusively produced Δ^{++} from the point of view of one-particle exchange. To this end we have investigated the behavior of the density matrix elements of the Δ^{++} as a function of the momentum-transfer squared t between the Δ^{++} and the target proton, and as a function of the energy of the X^- system, M_X. In addition, we have carried out a triple-Regge analysis in the kinematic region where the model is believed to be valid.

In contrast to the situation in inclusive Δ^{++} production in pp and $\pi^+ p$ reactions, the systems recoiling from the Δ^{++} in reaction (1) and in the reaction

$$K^- p \to \Delta^{++}X^{--} \tag{2}$$

are exotic and are not expected to contain resonances. Thus one expects Pomeron dominance at the upper vertex for both reactions (1) and (2). We have compared reaction (2) at 14.3 GeV/c (Ref. 6) to reaction (1) at 15 GeV/c in order to check this assumption. If factorization holds and Pomeron exchange dominates, these two reactions are related.

A study of inclusive Δ^{++} production in $\pi^+ p$ interactions at 100 GeV/c has shown that the process is consistent with one-pion exchange.[4] The average multiplicity in $\pi^+ \pi^-$ scattering was extracted by studying the system recoiling off the Δ^{++} produced in $\pi^+ p$ interactions. We have performed a similar study in which we extract the $\pi^- \pi^-$ average charged multiplicity and compare it to that of $\pi^+ \pi^-$.

The experimental details are presented in Sec. II. The cross sections for reaction (1) are given in Sec. III. Some inclusive distributions are shown
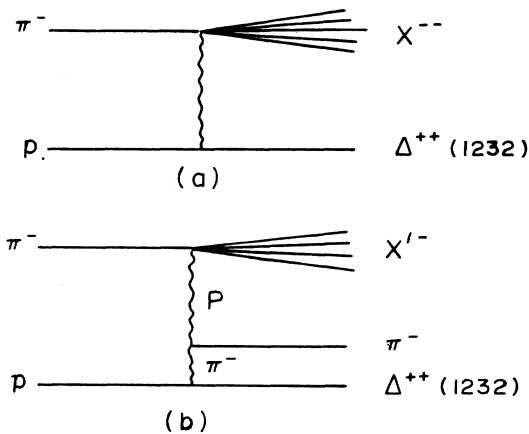
in Sec. IV, and a comparison with reaction (2) is carried out. Section V contains the results of the Δ^{++}-decay density matrix elements. In Sec. VI a triple-Regge analysis of the data is presented while in Sec. VII we discuss the average charged multiplicity of the system X^{--}. The results are summarized and conclusions are given in Sec. VIII.

II. EXPERIMENTAL DETAILS

The data used in the present study comes from an exposure of the 82-in. SLAC hydrogen bubble chamber to a 15-GeV/c π^- beam. About 470 000 pictures were taken, measured by the MIT PEPR (Precision Encoding and Pattern Recognition) system, and processed through the chain GEOMAT-SQUAW. Complete details about the event selection and processing criteria are given elsewhere.[8] All negative tracks were considered to be pions, while positive tracks with laboratory momentum less than 1 GeV/c could be unambiguously identified as pions or protons by ionization. From kinematic considerations we estimate that the detection efficiency for Δ^{++} production up to $|t| \lesssim 1.0$ (GeV/$c)^2$ is better than 90%. Each topology was corrected for scanning losses and measuring inefficiencies, the cross sections being obtained by normalizing all scanned events to the total $\pi^- p$ cross section at 15 GeV/c.[9]

With these criteria we can therefore conclude that our sample for the reaction

$$\pi^- p \to p\pi^+ + X^{--} \tag{3}$$

is reasonably unbiased if we restrict ourselves to $p\pi^+$ effective masses below 1.34 GeV/c and absolute momentum transfer squared from the $p\pi^+$ system to the target proton up to 1.0 (GeV/$c)^2$.

III. CROSS SECTIONS

The $p\pi^+$ mass distributions for $|t| < 1.0$ (GeV/$c)^2$ and $|t| < 0.6$ (GeV/$c)^2$ are shown in Figs. 2(a) and 2(b), respectively. A clear Δ^{++} signal is observed standing out on top of a smooth background in both, but the amount of background is less with the smaller t cut. However, the background in both cases can be almost completely removed by a cut on the proton polar angle, θ_J, in the Gottfried-Jackson frame for the $p\pi^+$ system, the distribution for which shows a strong forward-backward asymmetry. A study of this angular distribution above the Δ^{++} region shows that almost all events lie in the forward hemisphere. We therefore imposed the cut, $\cos\theta_J \leq 0$, and as can be seen in Figs. 2(c) and 2(d), this almost completely eliminates the background underneath the Δ^{++}.

In order to measure the cross section for reaction (1) with the two different momentum-transfer squared cuts, we fitted an expression of the

form

$$\frac{dN}{dM} = N\left[\alpha \, \frac{F_{BW}(m)}{\int F_{BW}(m)dm} + (1-\alpha) \, \frac{P(m)}{\int P(m)dm}\right] \tag{4}$$

to the distributions in Figs. 2(a) and 2(b). Here N is the total number of weighted events, α is the resonance fraction, $F_{BW}(m)$ stands for the Breit-Wigner function associated with the baryon resonance,[10] and $P(m)$ stands for a polynomial background.[11]

A minimum-χ^2 fitting procedure was used, allowing the parameters in Eq. (4) to vary. The best fits are represented by the solid lines in Figs. 2(a) and 2(b), and from them we calculate

$$\sigma(\pi^- p \to \Delta^{++}X^-, \quad |t| \leq 1.0 \text{ (GeV/}c)^2) = 0.85 \pm 0.04 \text{ mb}, \tag{5}$$

$$\sigma(\pi^- p \to \Delta^{++}X^-, \quad |t| \leq 0.6 \text{ (GeV/}c)^2) = 0.64 \pm 0.03 \text{ mb}.$$

In order to check the energy dependence of reaction (3), we have compared our results with those at 147 GeV/c[1] and at 205 GeV/c.[5] Figure 3 shows the cross section for reaction (3) for two sets of cuts: (a) $|t| < 1.0$ (GeV/$c)^2$ and $1.12 < M(p\pi^+) < 1.32$ GeV and (b) $|t| < 0.6$ (GeV/$c)^2$ and
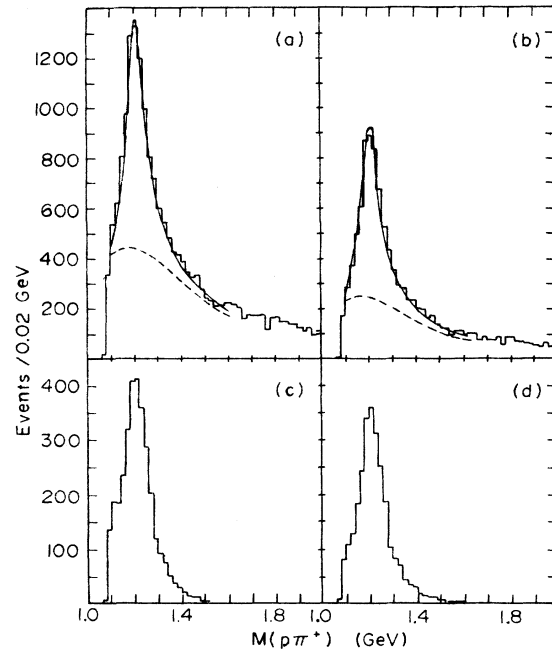

FIG. 2. Inclusive $p\pi^+$ mass distributions with the following cuts: (a) $|t\,p\,,p\pi^+| \leq 1.0$ GeV/$c)^2$, (b) $|t\,p\,,p\pi^+| \leq 0.6$ (GeV/$c)^2$, (c) $|t\,p\,,p\pi^+| \leq 1.0$ (GeV/$c)^2$ and $\cos\theta_J \leq 0$, (d) $|t\,p\,,p\pi^+| \leq 0.6$ (GeV/$c)^2$ and $\cos\theta_J \leq 0$. The solid line in (a) and (b) is the best fit to the data, as described in the text. The dotted lines are the contribution of background to the mass plot.
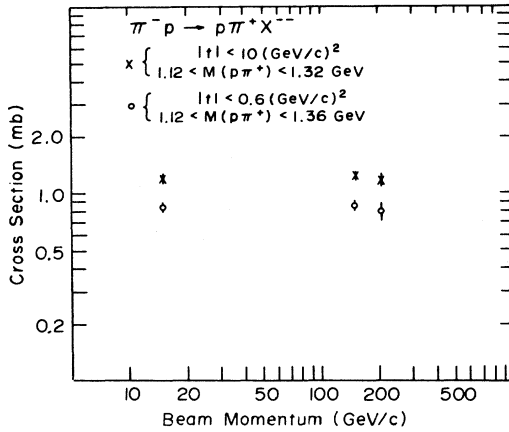
FIG. 3. The production cross section for the inclusive process $\pi^- p \to (p\pi^+) X^{--}$ as a function of the incident beam momentum.

$1.12 < M(p\pi^+) < 1.36$ GeV. As can be seen from this figure, the cross section for the $p\pi^+$ system produced in reaction (3) stays constant from 15 up to 205 GeV/c.

IV. PRODUCTION FEATURES OF Δ^{++}

A. t' distribution

Although $t' = |t - t_{\min}|$ is not a proper inclusive variable, it can be used to show the peripheral nature of the mechanism responsible for Δ^{++} production. In order to obtain the differential cross section $d\sigma/dt'$, the fits described in the previous section were repeated for each t' interval. In
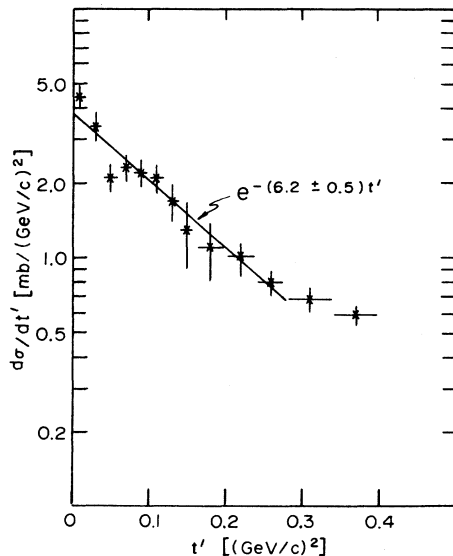
order to obtain an unbiased distribution up to $t' \leq 0.4$ (GeV/$c)^2$, the data was subject to an additional cut of $(M_X^2/s) \leq 0.3$. Figure 4 gives the resulting distribution which shows a steep exponential decrease. A fit to these data up to $t' = 0.28$ (GeV/$c)^2$ by a single exponential yields a slope of 6.2 ± 0.5 (GeV/$c)^{-2}$. This is to be compared to the value 5.3 ± 0.8 (GeV/$c)^{-2}$ obtained at 147 GeV/c.[1] For comparison we have also fitted the corresponding data of reaction (2) at 14.3 GeV/c for the same t' range. The resulting slope of 5.0 ± 0.5 (GeV/$c)^{-2}$ is in good agreement with the slopes obtained for the t' distribution in reaction (1).

B. P_T^2 distribution

The procedure used to obtain the transverse-momentum distribution $d\sigma/dp_T^2$ for the Δ^{++} is similar to that used for the $d\sigma/dt'$ distribution described above. In each of the P_T^2 intervals, a fit to the $p\pi^+$ mass distribution was carried out in order to get the amount of Δ^{++} produced in that interval. Figure 5 shows the $d\sigma/dP_T^2$ distribution for $P_T^2 \leq 0.45$ (GeV/$c)^2$. The distribution shows an exponential falloff with a slope of 7.0 ± 0.5 (GeV/$c)^{-2}$. This slope is similar to that obtained at 147 GeV/c, 6.7 ± 0.5 (GeV/$c)^{-2}$.[1]

C. Invariant cross section $d^2\sigma/dt d(M_X^2/s)$

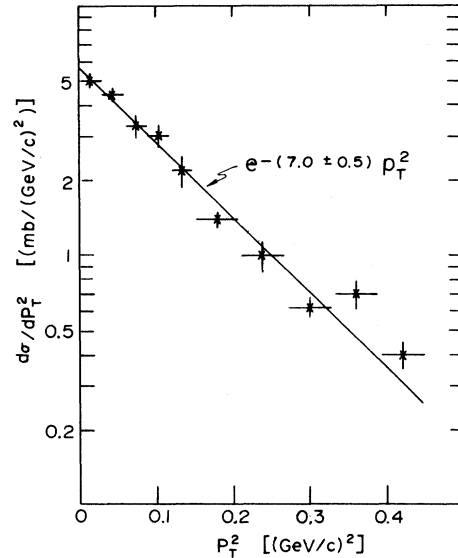In order to obtain the invariant cross section $d^2\sigma/dt d(M_X^2/s)$ for reaction (1), one would ideally

FIG. 4. The t' distribution for inclusive Δ^{++} production in $\pi^- p$ interactions at 15 GeV/c. A fit to an exponential form (solid line) yields a slope of 6.2 ± 0.5 (GeV/$c)^{-2}$.

FIG. 5. The P_T^2 distribution for inclusive Δ^{++} production in $\pi^- p$ interactions at 15 GeV/c. A fit to an exponential form (solid line) yields a slope of 7.0 ± 0.5 (GeV/$c)^{-2}$.

like to fit the $p\pi^+$ mass distribution for the amount of Δ^{++} in each of the t and M_x^2/s intervals. However, due to our statistics limitations and additional complications because of Chew-Low boundary effects, we used a different procedure. We have shown earlier (see Sec. II) that a cut on the proton polar angle, $\cos\theta_J \le 0$, reduced almost completely the background underneath the Δ^{++}. We have therefore defined the invariant cross section to be twice the density of points in the Chew-Low scatter plot $(t, M_x^2/s)$, after applying the cut $\cos\theta_J \le 0$ to the data, normalized to the cross section given in (5). The results are shown in Fig. 6 for the t range $0 \le |t| \le 0.6$ $(GeV/c)^2$. A triple-Regge analysis of these results is given in Sec. VI.

In this section we would like to compare our distribution with that of an experiment at 14.3 GeV/c studying reaction (2). In both reactions (1) and (2), the system recoiling against the Δ^{++} is exotic. Therefore, using duality considerations, one expects the exchanged-Reggeon–incident-pseudoscalar scattering to be Pomeron-dominated even at low M_x^2/s values. The dependence
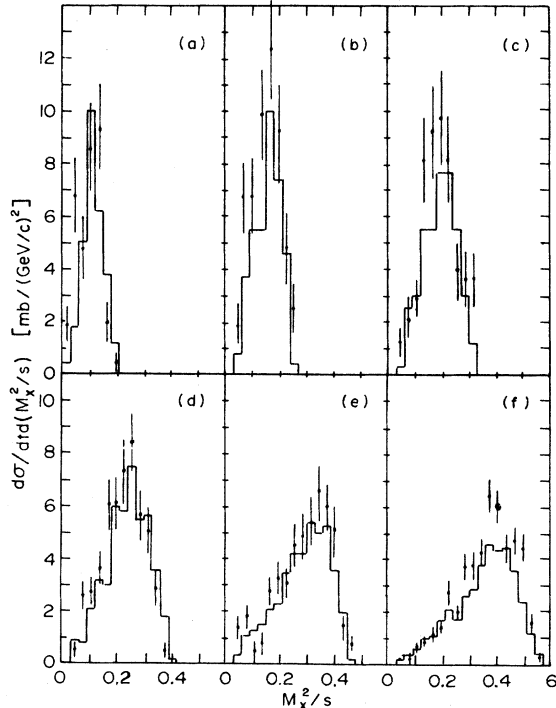

FIG.6. Invariant cross sections $d^2\sigma/dt d(M_x^2/s)$ for the reactions $\pi^- p \to \Delta^{++} + X^{--}$ at 14.3 GeV/c (histogram). For comparison, the $K^- p$ data was multiplied by 1.19, which is the ratio between the $\sigma_T(\pi^- p)$ and $\sigma_T(K^- p)$ at 50 GeV/c. (a) $0.05 \le |t| \le 0.10$ $(GeV/c)^2$, (b) $0.10 \le |t| \le 0.15$ $(GeV/c)^2$, (e) (c) $0.15 \le |t| \le 0.20$ $(GeV/c)^2$, (d) $0.20 \le |t| \le 0.30$ $(GeV/c)^2$, (e) $0.30 \le |t| \le 0.40$ $(GeV/c)^2$, (f) $0.40 \le |t| \le 0.60$ $(GeV/c)^2$.

of the inclusive cross section for reaction (1) on energy indeed supports this statement. Furthermore, if the Pomeron factorizes, one would expect the invariant cross sections for reaction (1) and (2) to be in the same ratio as the $\pi^- p$ and $K^- p$ total cross sections. Thus, we have multiplied the data of Ref. 6 by 1.19, which is the ratio $\sigma_T(\pi^- p)/\sigma_T(K^- p)$ at ~50 GeV,[9] and Fig. 6 shows the comparison of these data with ours. Although the two experiments are not at exactly the same s value and the systematic uncertainties have not been taken into account, the agreement between the two sets of experimental data is good. This indicates that our assumption of Pomeron dominance together with Pomeron factorization is a valid one.

V. Δ^{++} DECAY PROPERTIES

The decay properties of a produced resonance are frequently investigated by measuring the resonance density matrix elements. This task is often complicated, as in our case, by the presence of the background.

In this section we will investigate the behavior of the baryon resonance density matrix elements as a function of the inclusive variables t and M_x^2/s and we will restrict ourselves to the sample defined by $|t| \le 0.6$ GeV/c^2, $M_x^2/s \le 0.3$, and $m(p\pi^+) \le 1.34$ where, as discussed in Sec. II, our detection efficiency for Δ^{++} is 100% and the amount of background is small.

The technique that we have used has been successfully applied in an analysis of the reaction $K^- p \to \Sigma^+(1385)X^-$ at 4.2 GeV/c.[12] Using the maximum likelihood technique we fitted the mass dependence of the $(p\pi^+)$ t-channel helicity decay distribution assuming that the background under the Δ^{++} is in an s-wave state. We have therefore defined the following likelihood function:

$$\mathcal{L} = \alpha_R W(\theta, \phi) F_{BW}(m) + (1 - \alpha_R)P(m), \qquad (6)$$

where α_R is the resonance fraction, $F_{BW}(m)$ and $P(m)$ are as defined in Sec. III, and $W(\theta, \phi)$ is the decay angular distribution for the Δ^{++}. We have checked the quality of the fits by making χ^2 tests to the $p\pi^+$ effective mass distribution and the single-decay angular distributions. In Fig. 7 we show the result obtained for the density matrix element $\rho_{3/2,3/2}$ as a function of $|t|$ for different M_x^2/s values. Very similar results are obtained if instead of the above-described maximum likelihood method, we use only events with $\cos\theta_J \le 0$ and fit the backward hemisphere to the expression $(\frac{1}{4} + \rho_{3/2,3/2}) + 3(\frac{1}{4} - \rho_{3/2,3/2})\cos^2\theta$. As can be seen for all M_x^2/s values, $\rho_{3/2,3/2}$ is close to zero up to $|t| \sim 0.3$ $(GeV/c)^2$. The one-pion exchange mechanism predicts the value $\rho_{3/2,3/2} = 0$ for pure
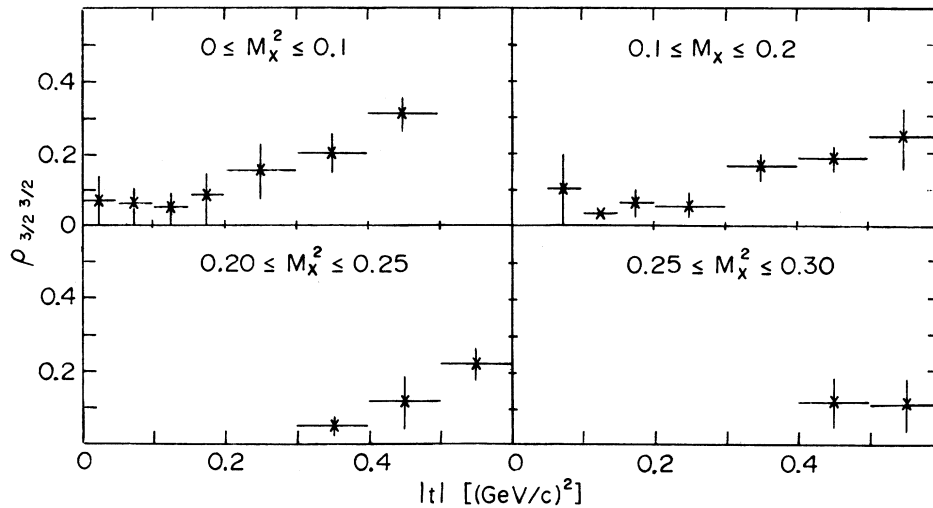
FIG. 7. The density matrix element $\rho_{3/2\,3/2}$ of the Δ^{++} as a function of $|t|$ for different M_X^2/s values.

pion exchange, or $\rho_{3/2,3/2} = 0.12$ for absorptive pion exchange.[13] We therefore conclude that the one-pion exchange mechanism is the dominant one for $|t| \leq 0.3$ (GeV/c)^2.

VI. TRIPLE-REGGE ANALYSIS

In this section we will attempt to describe Δ^{++} production in the framework of the triple-Regge model. The schematic diagram for this process is shown in Fig. 8. By E we denote the trajectory coupled to $p - \Delta^{++}$ vertex and by M we denote the exchange responsible for $\pi^- E \to \pi^- E$ scattering. From our discussion in Sec. IV C, we have reasons to expect M to be the Pomeron, while from our analysis in Sec. V on the Δ^{++} decay properties, we expect the pion to be the trajectory coupled to the p-Δ^{++} vertex. However, in our analysis we will rely only on the assumption that M is the Pomeron and try to obtain information on the exchange trajectory E. With this in mind, we write the triple-Regge invariant cross section as fol-
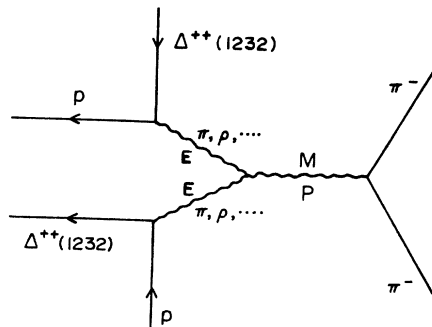

FIG. 8. Triple-Regge diagrammatic representation of the reaction $\pi^- p \to \Delta^{++} X^{--}$.

lows:

$$f(s, t, M_X^2/s) = \beta(t)(M_X^2/s)^{\alpha_P(0) - 2\alpha_E(t)} s^{\alpha_P(0) - 1},$$

(7)

where $\beta(t)$ is a residue function. $\alpha_P(0)$ is the intercept of the Pomeron trajectory for which we will use the value $\alpha_P(0) = 1.0$. This value has been used in similar triple-Regge analyses and in the one case[5] where it was left as a free parameter, $\alpha_P(0)$ was shown to be consistent with 1.0. $\alpha_E(t)$ is the trajectory of the exchanged particle E. In order to determine this trajectory, one generally fits expression (7) to the M_X^2/s distribution for various t intervals in the region where the model is valid ($M_X^2/s \leq 0.3$). However, in this case the differences between the kinematic boundaries in each t interval, due to the width of the Δ resonance, severely limits the allowed M_X^2/s region. In order to use the maximum number of events with $M_X^2/s < 0.3$, we followed the procedure described in Ref. 6 and defined the quantity $z = M_X^2/M_{max}^2$, where M_{max}^2 is the maximum possible value of M_X^2 for any given t and $p\pi^+$ mass value. We fitted the z distribution by the form $z^{b(t)}$, where $b(t) = \alpha_P(0) - 2\alpha_E(t) \simeq 1 - 2\alpha_E(t)$, at eight t values in the region, $0.05 \leq t \leq 1.0$ (GeV/c)^2. For this fit we used all events with $1.14 \leq M(p\pi^+) \leq 1.34$ GeV and $M_X^2/s < 0.3$. Figure 9 shows the results of this fit. In the same figure we show the expected trajectory for $E = \pi$ and for $E = \rho$. As expected from our density matrix analysis, for $t < 0.4$ (GeV/c)^2 the results are close to the π trajectory, while for larger t, they tend to move closer to the ρ trajectory. In order to check whether these results may be affected by the background events in the Δ-mass region, we repeated the fit with the additional cut of $\cos\vartheta_J < 0$. As seen from the
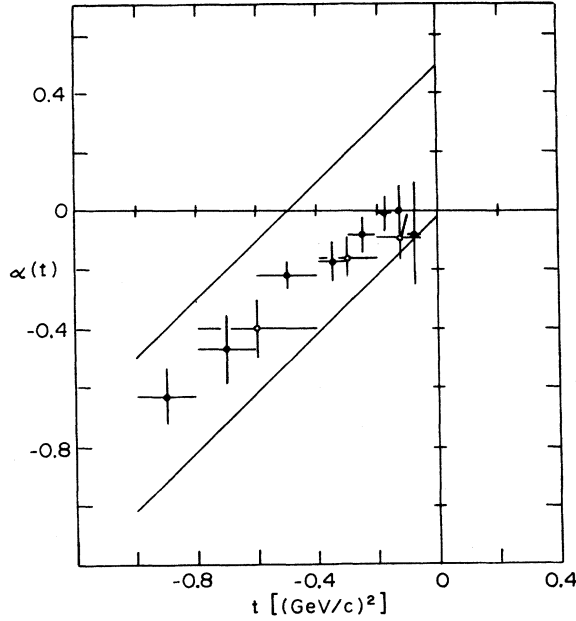
FIG. 9. Values of $\alpha_E(t)$ from a triple-Regge fit for the reaction $\pi^-p \to (p\pi^+)X^{--}$ at 15 GeV/c. The full dots are from fits to the data with the cuts $|t| \leq 1.0$ (GeV/c)^2, $M_X{}^2 \leq 0.3$, and $1.14 \leq M(p\pi^+) \leq 1/34$ GeV. The open circles have the additional cut of $\cos\theta_J \leq 0$.

figure, the results remain unchanged.

Our results agree with those obtained in K^-p interactions at 14.3 GeV/c^6 and are in contradiction with the similar analysis of inclusive Δ^{++} production in π^-p and K^-p interactions at 10 and 16 GeV/c.[5] We would like, however, to point out that our results are dependent on the assumption that $\alpha_p(0) = 1$.

VII. AVERAGE CHARGED MULTIPLICITY

Assuming the pion to be the dominant exchange for $|t| < 0.4$ (Gev/c)^2, the system X^{--} in reaction (1) is the result of an off-mass-shell pion interacting with a real pion. In other words, we "measure" the reaction

$$\pi_E^- \pi^- \to X^{--}, \tag{8}$$

where π_E^- stands for the off-mass-shell pion. Therefore, a study of the average charged multiplicity of X^{--}, $\langle n_X \rangle$, as a function of $M_X{}^2$ would yield information about the $\pi^-\pi^-$ average charged multiplicity. However, when one calculates the average charged multiplicity of a reaction $ab \to X$, one does not include events in the elastic channel, $ab \to ab$. In our case this would mean that we have to remove the reaction $\pi^-p \to \Delta^{++}\pi^-\pi^-$ (four-prong, four-constraint events, 4P-4C) from the sample for the $\langle n_X \rangle$ study.

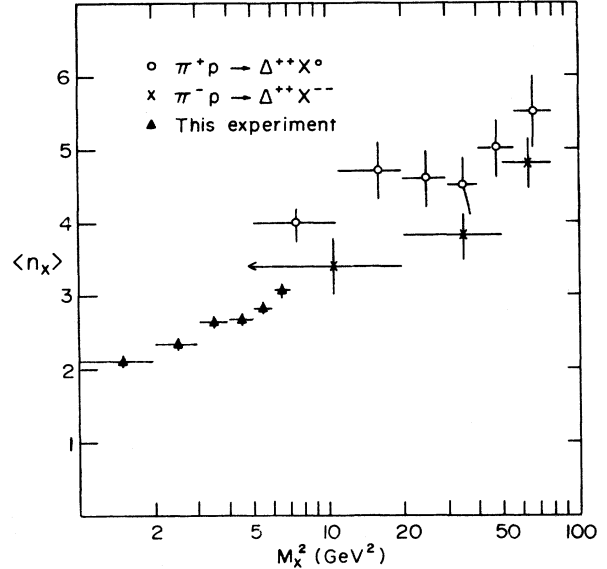Figure 10 shows the results obtained for

FIG. 10. Comparison of the average charged multiplicity of the system recoiling against the Δ^{++} in π^+p interactions at 100 GeV/c (see Ref. 4) and in π^-p interactions at 147 GeV/c (see Ref. 14) and at 15 GeV/c.

$\langle n_X(M_X{}^2) \rangle$ at 15 GeV/c together with results from a similar analysis studying reaction (1) at 147 GeV/c.[14] We have plotted for comparision data obtained from the reaction

$$\pi^+p \to \Delta^{++}X^0 \tag{9}$$

at 100 GeV/c.[4] For all three energies, the 4P-4C events are excluded. For the π^- reaction $|t| < 0.4$ (GeV/c)^2, while for the π^+ reaction $|t| < 0.88$ GeV/c)^2. A study of $\langle n_X(M_X{}^2, t) \rangle$ at 147 GeV/c shows almost no t dependence of $\langle n_X \rangle$; therefore, the comparison of these two reactions is plausible. As evident from Fig. 10, charged multiplicity of the X^0 system in reaction (9) is consistently higher by about 0.5 than that of the X^{--} system in reaction (1). Since the 100-GeV/c π^+ experiment also concluded that its results are consistent with one-pion exchange, our comparison indicates that the $\pi^+\pi_E^-$ average charged multiplicity is higher than the $\pi^-\pi_E^-$ one by about 0.5.

For a further interpretation of this result, it is useful to refer to a simple model which was used to explain differences of average charged multiplicities in a study of π^-p interactions at 147 GeV/c.[15] In this model the average charged multiplicity $\langle n_X \rangle$ of the reaction $a + b \to c + X$ may be expressed in the form (see Fig. 11)

$$\langle n_X \rangle = n_{E_{ac}} + n_0 + n_b. \tag{10}$$

n_0 is the average charged multiplicity in the central region and is believed to increase linearly with $\ln M_X{}^2$. $n_b(n_{E_{ac}})$ is the average number of particles
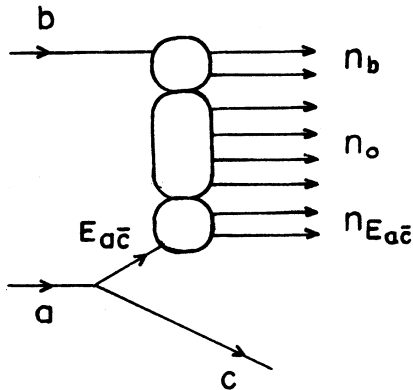
FIG. 11. Diagrammatic representation of the reaction $a+b \to c+X$.

into which particle b (E_{ac}, the exchanged particle at the ac vertex) fragments. Therefore, in view of this model, the difference between $\langle n_x \rangle$ from reaction (9) and $\langle n_x \rangle$ from reaction (1) would be $n_{\pi^+} - n_{\pi^-}$. Thus, in the framework of this model, we conclude that the π^+ fragements on the average into more particles than the π^-. In order to check the consistency of this result, one should compare $\langle n \rangle$ for π^+p to that for π^-p. An extensive study of $\langle n \rangle$ for different reactions and a wide range of energies[16] shows indeed that $\langle n(\pi^+p) \rangle$ is higher by 0.0 to 0.4 than $\langle n(\pi^-p) \rangle$. The same trend is also apparent in Kp reactions, the K^+p average charged multiplicity being higher than that of K^-p.[16]

VIII. SUMMARY AND CONCLUSIONS

In a study of Δ^{++} inclusive production in π^-p interactions at 15 GeV/c, we have measured its production cross section and obtained the values

$$\sigma(\pi^-p \to \Delta^{++}X^-), \quad |t| < 1 \ (\text{GeV}/c)^2) = 0.85 \pm 0.04 \ \text{mb}$$

and

$$\sigma(\pi^-p \to \Delta^{++}X^{--}), \quad |t| < 0.6 \ (\text{GeV}/c)^2) = 0.64 \pm 0.03 \ \text{mb}.$$

We have studied the production mechanism in a one-particle-exchange picture, trying to determine the nature of the exchanged particles. We have shown that the Pomeron is the dominant exchanged particle at the upper vertex by studying the energy dependence of reaction (1) and by comparing it to reaction (2) at 14.3 GeV/c. This comparison assumed Pomeron factorizability and our results support the validity of this assumption.

From a study of the decay distribution of the Δ^{++} we have concluded that for $|t| \leq 0.3 \ (\text{GeV}/c)^2$ one-pion exchange is the dominant mechanism. The steep t' and P_T^2 distributions observed are in agreement with this last statement. The same conclusions are drawn from a triple-Regge analysis where we found the effective trajectory to be close to the π trajectory at small t and near the ρ trajectory at higher t. We have studied the average charged multiplicity of the X^{--} system of reaction (1). Comparing our data with data for this reaction at 147 GeV/c, as well as data for reaction (9) from a 100-GeV/c experiment, we were led to conclude that the $\pi^+\pi^-$ average charged multiplicity is higher than that of $\pi^-\pi^-$. This also seems to be the case for πp (Kp) interactions, the π^+p (K^+p) being higher than the π^-p (K^-p) average charge multiplicity.

*On leave of absence from Tel Aviv University, Israel.

†Present address: Tel Aviv University, Israel.

‡Present address: Weizmann Institute of Science, Israel.

§Present address: Fermilab, Batavia, Illinois.

[1]D. Brick et al., report, 1977 (unpublished).

[2]I. Ohba and A. Nakamura, Prog. Theor. Phys. 53, 1786 (1975); 54, 1235 (1975).

[3]F. T. Dao et al., Phys. Rev. Lett. 30, 34 (1973); J. P. De Brion et al., Phys. Rev. Lett. 34, 910 (1975); S. J. Barish et al., Phys. Rev. D 12, 1260 (1975).

[4]J. Erwin et al., Phys. Rev. Lett. 35, 980 (1975); J. V. Beaupré et al., Nucl. Phys. B67, 413 (1973).

[5]P. Borzatta et al., Nuovo Cimento 15A, 45 (1973); P. Bosetti et al., Nucl. Phys. B81, 61 (1974).

[6]A. C. Borg et al., Nuovo Cimento 34A, 21 (1976).

[7]D. Brick et al., Phys. Rev. Lett. 31, 488 (1973).

[8]D. Brick, Ph.D. thesis, M. I. T., 1973 (unpublished); P. A. Miller, S. M. thesis, M. I. T., 1974 (unpublished).

[9]E. Bracci et al., Reports Nos. CERN/HERA 72-1 and 72-2 (unpublished).

[10]
$$F_{\text{BW}}(m) = \frac{m \, \Gamma}{(m^2 - m_0^2)^2 + m_0^2 \, \Gamma^2}, \quad \Gamma = \Gamma_0 (q/q_0)^3.$$

[11]
$$P(m) = 1 + \sum_{i=1}^{6} A_i (m - m_p - m_{\pi^+})^i.$$

[12]F. Barreiro *et al*., Report No. CERN/EP/PHYS 76-23

(unpublished).

[13]E. Gotsman, Phys. Rev. D <u>9</u>, 1575 (1974).

[14]I. H. S. Consortium, unpublished work.

[15]D. Fong *et al*., Phys. Rev. Lett. <u>37</u>, 736 (1976).

[16]E. Albini *et al*., Nuovo Cimento <u>32A</u>, 101 (1976).